

Speed behaviour upon approaching freeway curves

Vos, Johan; Farah, Haneen; Hagenzieker, Marjan

DOI

[10.1016/j.aap.2021.106276](https://doi.org/10.1016/j.aap.2021.106276)

Publication date

2021

Document Version

Final published version

Published in

Accident Analysis and Prevention

Citation (APA)

Vos, J., Farah, H., & Hagenzieker, M. (2021). Speed behaviour upon approaching freeway curves. *Accident Analysis and Prevention*, 159, 1-13. Article 106276. <https://doi.org/10.1016/j.aap.2021.106276>

Important note

To cite this publication, please use the final published version (if applicable).
Please check the document version above.

Copyright

Other than for strictly personal use, it is not permitted to download, forward or distribute the text or part of it, without the consent of the author(s) and/or copyright holder(s), unless the work is under an open content license such as Creative Commons.

Takedown policy

Please contact us and provide details if you believe this document breaches copyrights.
We will remove access to the work immediately and investigate your claim.



Speed behaviour upon approaching freeway curves

Johan Vos^{*,1}, Haneen Farah², Marjan Hagenzieker³

Department of Transport and Planning, Faculty of Civil Engineering and Geosciences, Delft University of Technology, Stevinweg 1, 2628 CN Delft, The Netherlands

ARTICLE INFO

Keywords:

Freeway curve anticipation
High Frequency Floating Car Data
Speed profiles
Sight distances

ABSTRACT

The actual speed behaviour when drivers approach a curve is very relevant to assess the road design and safety but is mostly overlooked in the scientific literature. Most research into curve driving behaviour is focussed at the behaviour inside the curve, although the speed selection is done before curve entry. The main objective of this research is to identify which freeway characteristics play a role in driving speed selection. High Frequency Floating Car Data, detailed reconstruction of the curves and their surroundings, as well as three dimensional sight distance analysis, were used to analyse individual speed profiles on 153 Dutch freeway curves. By defining the positions where the acceleration approaches 0 m/s^2 before and after a curve starts, the positions when the driver started and stopped decelerating upon curve entry were defined. Further correlation and regression analysis of those positions revealed that the radius of the curve is indeed a main explaining variable, as well as the speed driven before deceleration starts. Sight distances and cross section characteristics play a further role in determining the position where deceleration starts. Deceleration ends at approximately 135 m after curve start, and the speed in a curve is also correlated with the deflection angle and length of a curve. Sight distances do not play a role in selecting the speed in a curve based on this research. Overall, the findings indicate a non-constant nature and variability of speed behaviour upon curve entry. This can be used for safer freeway curve design and to assess traffic safety based on actual speed behaviour.

1. Introduction

The speed which drivers select to drive in a freeway curve is of major influence on traffic safety. A speed which is too high, results in a loss of control of the vehicle due to a loss of friction (Donnell et al., 2016; Himes et al., 2019; Li and He, 2016). Because of this, the design of freeway curves has mostly been related to side friction factors (Fitzpatrick and Kahl, 1992). Human factors are however mostly overlooked in curve design, although it is the driver who selects the speed (Charlton and Starkey, 2017b). Understanding how drivers select their driving speeds is therefore of importance to safe freeway curve design.

Research in curve driving has mainly focussed on driving aspects when the driver is already inside the curve. Such research focusses on where drivers look (Gruppelaar et al., 2018; Land and Lee, 1994; Lehtonen et al., 2014; Salvucci and Gray, 2004; Shinar et al., 1977), the lateral position inside the lane (Coutton-Jean et al., 2009; de Waard et al., 2004; Van Winsum and Godthelp, 1996) or the speed drivers select

in a curve (Farah et al., 2019; Hassan et al., 2011a, 2011b; Luque and Castro, 2016; Odhams and Cole, 2004). Only a few research studies have focused on the curve detection phase (Lehtonen et al., 2012), even though task descriptions state that the period just before entering the curve is most important in the perceptual, cognitive and psychomotor tasks drivers need to select their driving speeds in a curve (Campbell et al., 2012; McKnight and Adams, 1970; Shinar, 2017). Explorative research showed that drivers take the entire curve surroundings into account while selecting their speed when entering a curve (Vos et al., 2020). It remains unclear however, which cues are of importance to the driver.

The key feature of a curve is its radius. A relatively small radius urges drivers to slow down, in order not to skid (Donnell et al., 2016; Gibson and Crooks, 1938). This means that the radius is a key element upon which drivers select their speed. Because the driving task is mostly visual (Hills, 1980; Sivak, 1996), drivers need to perceive the radius. However, from a driver standpoint the perception of a curve gets distorted in a

* Corresponding author.

E-mail addresses: J.Vos-1@tudelft.nl (J. Vos), h.farah@tudelft.nl (H. Farah), M.P.Hagenzieker@tudelft.nl (M. Hagenzieker).

¹ <https://orcid.org/0000-0001-5954-967X>.

² <https://orcid.org/0000-0002-2919-0253>.

³ <https://orcid.org/0000-0002-5884-4877>.

hyperbola, which results into less well perceived curvature when the radius decreases (Brummelaar, 1975). Because it is difficult for drivers to perceive the curve radius, other factors are assumed to play a role in curve perception and speed selection such as the deflection angle of a curve (Fildes and Triggs, 1985; Riemersma, 1988; Wang and Easa, 2009). Studies on distortion in the perception of curvature were mostly based on perspective drawings as laboratory stimuli and lack therefore other static and dynamic curve characteristics (e.g., guardrail, signing or traffic). Some of these elements have however been validated in experiments or field studies, these include the transition curve (Perco, 2006; Riemersma, 1989) and vertical sag curves (Bella, 2015; Campbell et al., 2012; Wang and Easa, 2009). Visual research using eye trackers shows more visual attention towards the right, in right turning curves than to the left in left turning curves (Lappi and Lehtonen, 2013; Shinar et al., 1977), suggesting right turning curves need more attention. In both laboratory studies (Singh and Fulvio, 2007) and simulator studies (Coutton-Jean et al., 2009), it was shown that drivers use and need continuous information to assess the curvature. This includes road markings (Charlton and Starkey, 2013; Coutton-Jean et al., 2009; de Waard et al., 2004), curve signs (Charlton, 2004), road lighting and tree lines (Blumentrath and Tveit, 2014). These elements need to be visible enough though, otherwise drivers decelerate later and more sharply before curve entry (Jamson et al., 2015). Partly occluded shapes however, can still be interpreted based on knowledge about these objects (Hazenbergh and van Lier, 2016). Indeed, when drivers are familiar with the road, they choose higher speeds (Wu and Xu, 2018). Drivers also choose their speed based on perceived road categories (Charlton and Starkey, 2017a) and the number of lanes present (Calvi et al., 2018), so the composition of the cross section is also relevant to the driver. Furthermore, design consistency studies showed that the tangent characteristics upstream of the curve, such as tangent length and width, influence the speed reduction (Hassan et al., 2011a, 2011b).

Speed profiles give more insights into speed development upstream of a curve and in the curve itself and can be considered as key input for assessing the way drivers drive through curves (Dias et al., 2018). Research into speed profiles showed that the speed is not constant in a curve (Bella, 2014; Montella et al., 2015; Wang et al., 2020), and that deceleration starts before the curve and ends inside the curve. Since drivers start to search for the upcoming curve and start to decelerate before the curve (Campbell et al., 2012; Hallmark et al., 2015; Land and Lee, 1994; Lehtonen et al., 2012; Shinar et al., 1977), the speed profile before a curve is of interest in investigating which of the elements discussed above may be of importance to the driver in speed selection. There is still a knowledge gap on this point. Since the deceleration stops within the curve, the speed selection inside the curve is also of interest to analyse the speed behaviour upon curve approach.

Therefore, the aim of this research is to gain insights into which elements are of influence on the speed profile when approaching a curve, and the speed selection in a curve. In order to gain these insights the following research questions were defined:

- Where do drivers begin to decelerate in reference to the curve start? And which elements influence this position?
- Which speed do drivers adopt in a curve? And which elements influence this speed?

The following section will discuss the research methods used to answer these questions. Section 3 analyses the data in three steps: first insights into speed profiles, correlations of speeds and curve characteristics, and regression analysis. Sections 4 and 5 discuss the results and summarize the conclusions, respectively.

2. Research method

In order to investigate the relationship between speed profiles and curve characteristics, we chose real world situations over laboratory

settings such as simulators, to avoid any bias due to lack of motion cues or limitations in the dynamic visualisation of the road scenario (Bella, 2009; Molino et al., 2005). We therefore selected a representative sample of freeway curves and obtained relevant and measurable curve characteristics.

2.1. Curve selection

We chose our curves based on a number of characteristics that are known from literature to have an influence on speed selection. Therefore, a representative selection of deflection angles, curve radii and number of lanes were considered in the freeway curves selection. Speed on off-ramps is much influenced by slowing down for the junction at the end of it, so off-ramps are excluded in the selection. Only main carriageways and connector roads in junctions were included.

This resulted in a selection of 99 road sections which include 153 curves, as presented in Fig. 1 with their main characteristics. The curves were selected throughout The Netherlands as presented in Fig. 2.

2.2. Obtaining relevant curve characteristics

All of the selected curves were reverse engineered in order to have insights into the relevant geometric elements: horizontal alignment (radius, transition curves, deflection angles and tangents), vertical alignment (grades, sag and crest curves) and cross section elements (width of carriageway, number of lanes, presence of hard shoulder, superelevation, distance from side marking to guardrail).

Using the reverse engineered road alignments, sight distances were obtained every 10 m using the Dutch “Zicht” application (Broeren, 2002) which was developed for Rijkswaterstaat (Dutch Directorate-General for Public Works and Water Management) and used for more than 20 years. In three dimensional models of the curve environment, guiding elements (which run parallel to the alignment of the curve), were identified per curve. This included the roadway itself, brake-lights (stopping sight distance), guardrail, treelines, noise barriers and curve signs as guiding elements. The position of these guiding elements was fed into “Zicht”. The program stops every 10 m along the alignment, to position a red box at the predefined offset every 5 m in front of the driver and checks whether or not it is visible from the driver standpoint. Fig. 3 shows a graphical example of this analysis which resulted in a definition of maximum sight distances for each guiding element, at every 10 m along the alignment. Results from “Zicht” have been validated using dashcam video’s, as shown in Fig. 3.

2.3. Speed data collection and preparation

Continuous speed profiles provide detailed information about speed development during the curve anticipation phase (Dias et al., 2018), and overcome traditional errors derived from classic point speed measurements (Hassan et al., 2011a, 2011b; Wang et al., 2020). To create these speed profiles along the generated alignments, High Frequency Floating Car Data from Flitsmeister-users was used. This smart-phone navigation app is used by 1.6 million users in The Netherlands, of which most are personal car or van drivers. Regular Floating Car Data cannot be used to create speed profiles, but only to show speed distributions per section of road (Colombaroni et al., 2020). For this study, the data gathering algorithms for the app were set to a frequency of 1 Hz along the selected road sections. Data collection was executed in March, April and September 2020. These are unique speed-profiles per trip, from which acceleration-profiles can be derived. The amount of precipitation was also added for each speed profile, using the Dutch climatological radar rainfall dataset (Saltikoff et al., 2019) in order to study relations between speed and wet road conditions.

The use of speed profiles containing speed and deceleration per second allows us to find positions in the speed profile where the slope of speed versus time changes, which are called breakpoints. This method

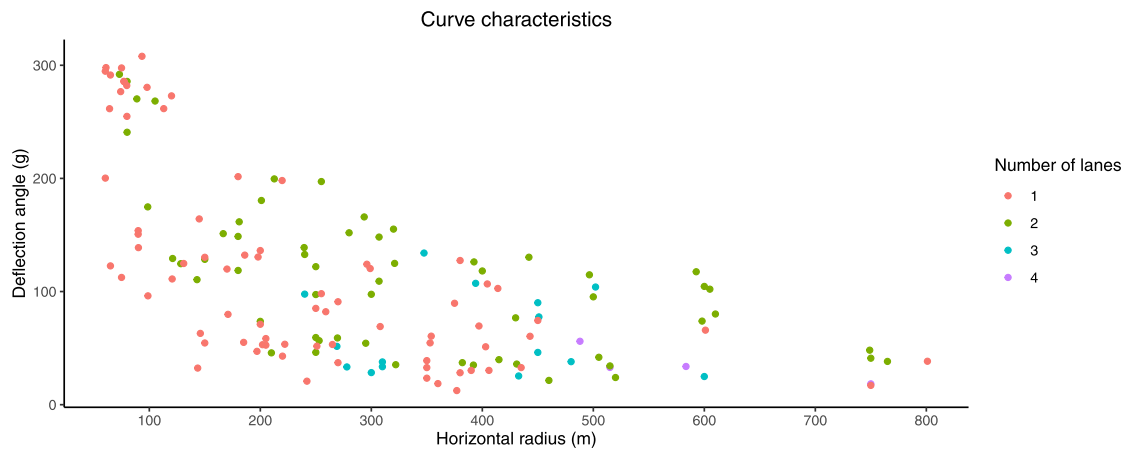


Fig. 1. Scatterplot of main characteristics of the selected curves in this study.

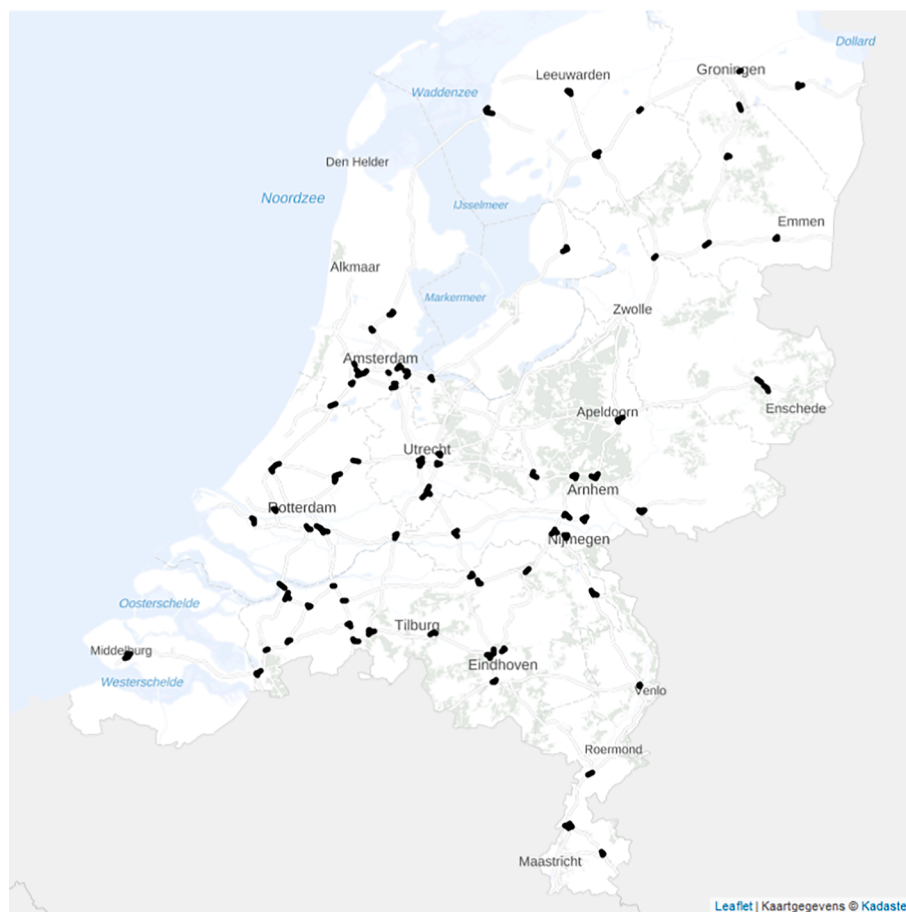


Fig. 2. Map showing the location of the curves in The Netherlands (in black).

was introduced by Montella et al. (2015), who also showed that deceleration starts in front of the curve, and ends inside the curve. Breakpoints are the main points of interest in this research, and are explained further in Fig. 4. The positions of breakpoint 1 (BP1) and breakpoint 2 (BP2) are defined based on the acceleration profile. The position where the continuous radius starts is the reference point for the breakpoints positions (zero). The point upstream of a curve start, where the acceleration approaches 0 m/s^2 , is defined as BP1 and has a negative position. The point downstream of the curve start, where the acceleration approaches 0 m/s^2 , is defined as BP2 and has a positive position. The

acceleration profile was smoothed using the LOESS algorithm in R (Cleveland et al., 1992) to obtain a more realistic acceleration profile. Because of this smoothing, hardly any point will have an exact acceleration of 0 m/s^2 . Therefore thresholds needed to be set to find the point closest to 0 m/s^2 . Using a threshold of 1 s in which the acceleration profile is between -0.1 m/s^2 and 0.1 m/s^2 shows an optimal result for defining the positions of the breakpoints.



Fig. 3. On the left the analysis of “Zicht” on the visibility of the curve signs. The red object in the 3D model is the object “Zicht” checks along the alignment, in this case a curve sign, positioned above the guardrail (the dark grey line). On the right, this exact viewpoint is shown in the real life situation. (For interpretation of the references to colour in this figure legend, the reader is referred to the web version of this article.)

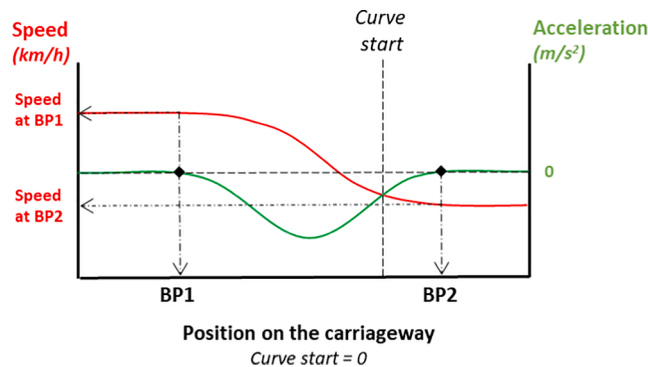


Fig. 4. Theoretical speed and acceleration profiles drawn around the curve start.

2.4. Speed data filtering

All road sections were checked for road-works during the measuring period. Road works could entail extra signing, lowering speeds or distracting elements along the road. In order not to bias the outcomes in that direction, trips during roadworks were eliminated from the database.

Since we are interested in the speed selection based on curve characteristics, car following behaviour should be eliminated from the database. Every road segment in The Netherlands has a loop-detector which measures all traffic and generates average speeds and traffic volumes per minute. Hashim (2011) showed that above a headway of 5 s, most vehicles travelled at their desired speed. This is called a free-flow situation. Given that traffic flow is Poisson distributed, the headway is exponentially distributed. Taking an average headway of 5 s, the chance is around 5% that a vehicle has a headway greater than 15 s ($e^{-(15/5)} = 0.0497$). This is 4 vehicles per minute. In order to select trips which have a probability of 95% to have been in free-flow, trips in periods with 5 or more vehicles per minute per lane were filtered out of the database.

This results in 996,375 unique trips available in this research, on average 10,064 trips per road section (sd = 8,616, max = 41,041, min = 425). This large variability is explained because some road sections are situated in busy urban areas, and other curves are situated in remote rural areas, see also Fig. 2. Some road sections also had many trips filtered out because of roadworks being present during the measurements.

Based on the loop detector data, we were able to compare our sample in the High Frequency Floating Car Data to the entire population. On average, our sample contains 9.1% (sd 7.1%) of all the drivers in the selected periods without roadworks and in free-flow. By comparing the average speeds of all the drivers, based on the loop detector data, to the sample data, it was found that the drivers in our sample drove on average 5.4 km/h faster (sd 4.9 km/h) at the loop-detector than all the drivers in the same free-flow periods. Based on the measurements of

Farah et al. (2019) the sample in this research represents on average around the 60th percentile of all the drivers.

3. Data analysis

The following sub-sections describe the analyses of the data in three steps: first we show some insights into speed profiles (3.1), then correlations of speeds and curve characteristics were investigated (3.2), and finally the results of the regression analysis for predicting the positions and speeds of BP1 and BP2 are presented (3.3).

3.1. First insights into speed profiles

In order to get a first feel of the collected data, speed profiles of curves with radii around 250 m were compared. For these curves the median speed profile was calculated, by calculating the median speed for every meter considering all individual speed profiles. All these curves have relative tangent approaches. So, based on common speed prediction models, it is expected that all these curves have almost equal profiles (Hassan et al., 2011a, 2011b). Fig. 5 however shows some different characteristics in the speed profiles and breakpoints. This leads us to the hypothesis that other curve characteristics than curve radius alone might explain these differences. And indeed, when looking at the dashcam pictures in Fig. 6, we see different road layouts in terms of different cross sections and surroundings.

3.2. Correlations of speed, deceleration and positions of breakpoints 1 and 2 to curve characteristics

The positions of BP1, BP2 together with the speeds at BP1 and BP2 are identified as variables which determine the speed profiles. The average deceleration is derived from those two points. Correlation analysis between these five variables with curve geometry and sight distances are presented in Fig. 7. In Fig. 7 only variables which have at least one correlation coefficient above 0.25 or below -0.25 are shown. All shown correlation coefficients have a significance of $p < 0.001$. The variables ‘Curvature Change Rate’, ‘Deflection angle’ and ‘Length of curve’ include both the transition curves and circular curve. The ‘number of usable lanes’ are the available lanes to the driver, either all available lanes on a carriageway, or the available lanes to pre-sort in the direction of the curve. The ‘Ratio A to R’ represents the value of A-value of the clothoid divided by the horizontal radius in meters, and is therefore related to the length and angle of the transition. The ‘visible angle’ is defined as the amount of angle which is visible based on any parallel guiding element, as explained in Vos et al. (2020) and the ‘visible length’ is the amount of length of the curve which is visible. All individual speed profiles have been used in the correlation analysis in order to account for individual differences in speed profiles and their respective positions of the breakpoints. Even though Fig. 7 does not show correlation coefficients above 0.5 or below -0.5 , some general conclusions can be drawn, even though speed prediction models usually

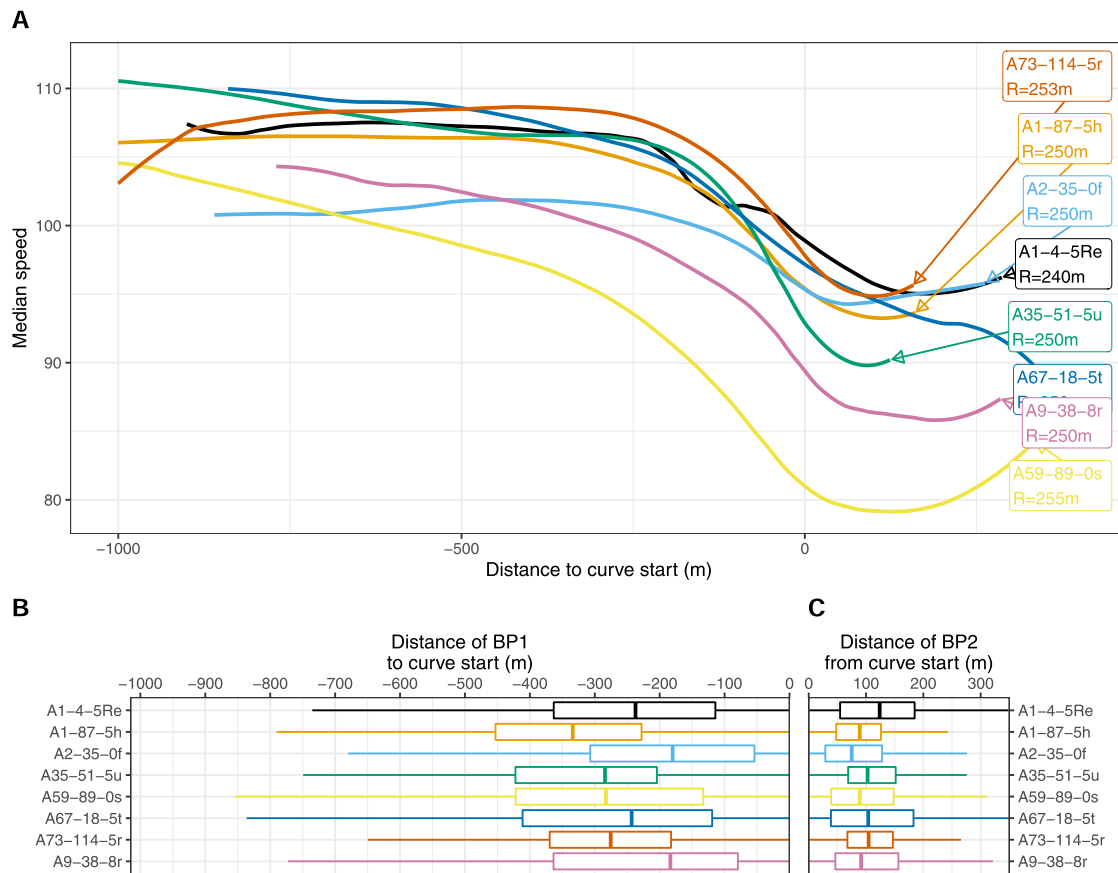


Fig. 5. Speed profiles of eight curves with radii around 250 m and information about their breakpoints. A) shows the profiles of median speeds of all measured speeds per curve, relative to the start of the curve radius. A note to profile “A1-4-5Re”, which shows a bump between 250 and 50 m before the curve start. This bump is probably due to an overpass of around 110 m at this location, which caused GPS inconsistencies. B) shows boxplots of the position of BP1 per curve. C) shows boxplots of the position of BP2 per curve.

only report correlation coefficients above 0.4 when using multiple variables (Hassan et al., 2011a, 2011b; Llopis-Castelló et al., 2018). Since we have used all individual speed profiles in our analyses and analyse single variables, we expect relative low correlations. In behavioural sciences a correlation coefficient between 0.3 and 0.5 is defined as “medium”, below 0.3 as “low”, and above 0.5 as “strong” (Cohen, 1988). Distance of BP1 to the curve start, average deceleration and the speed at BP2 show the largest correlations with curve geometrics and sight distances.

The speed at BP2 seems to be correlated with the speed at BP1, suggesting a relation between speed outside and inside a curve. Speed at BP1 is also correlated with the position of BP1, which is to be expected: faster driving needs more deceleration length. Sight distances on guiding elements are also correlated with the position and speed at BP1: when present, guiding elements such as closed elements (e.g., noise barriers) or curve signs have a higher correlation with the position and speed at BP1 than stopping sight distance or road sight distance. The variable that is most correlated with the distance of BP1 is however the visible length of the curve.

Speed at BP2 is correlated more to the curve geometric elements such as Curvature Change Rate (CCR), deflection angle, horizontal radius, transition curve and number of lanes. A relative large correlation can also be observed between the speed at BP2 and the maximum speed sign and presence of curve signs. Also the sight distance available on guiding elements is correlated with the speed in a curve. The position of BP2 is hardly correlated with anything, suggesting that geometric elements and sight distances do not influence the position of BP2. The average deceleration is correlated with the same geometric elements as the speed

at BP2. Average deceleration however seems to be more correlated with sight distance on the guiding elements than the speed at BP2 does.

In the above paragraphs we have discussed the correlations in Fig. 7. These all met the threshold of a correlation coefficient above 0.25 or below -0.25 . It is also of interest to see which variables did not meet this threshold. The introduction mentioned that the curve direction influences driver behaviour, but this was not found in this analysis shown Fig. 7. Also sag curves in combination with the horizontal curve were mentioned to influence driver perception, but this did not show in Fig. 7. Superelevation is of major importance in using design speeds to design a curve, however it did not correlate to any of the breakpoints. Road categories were also identified in the introduction to influence the driver. Since only freeways were examined, we focussed instead on types of discontinuity. Discontinuities are transitions between two road-sections which limits the amount of lanes available for a driver in a certain direction because of pre-sorting. However, the different types of discontinuities did not correlate to any of the breakpoint variables. The number of usable lanes in the direction of the curve at a discontinuity takes pre-sorting into account, and even usable lanes are less correlated with BP1 than all lanes in the cross section at BP1. So, no direct correlation of discontinuity or pre-sorting with BP1 and BP2 variables was found. Most of the sight distances to guiding elements were satisfactorily correlated with the breakpoints. The positions from which sight on the curves start, or where the first 100 m of the curve is available to the driver, however did not correlate at all with BP1 or BP2 variables. And only the presence of curve signs as guiding elements seemed to correlate to the breakpoints; guardrail, treelines or closed elements did not. Finally, external weather effects such as daylight and precipitation also

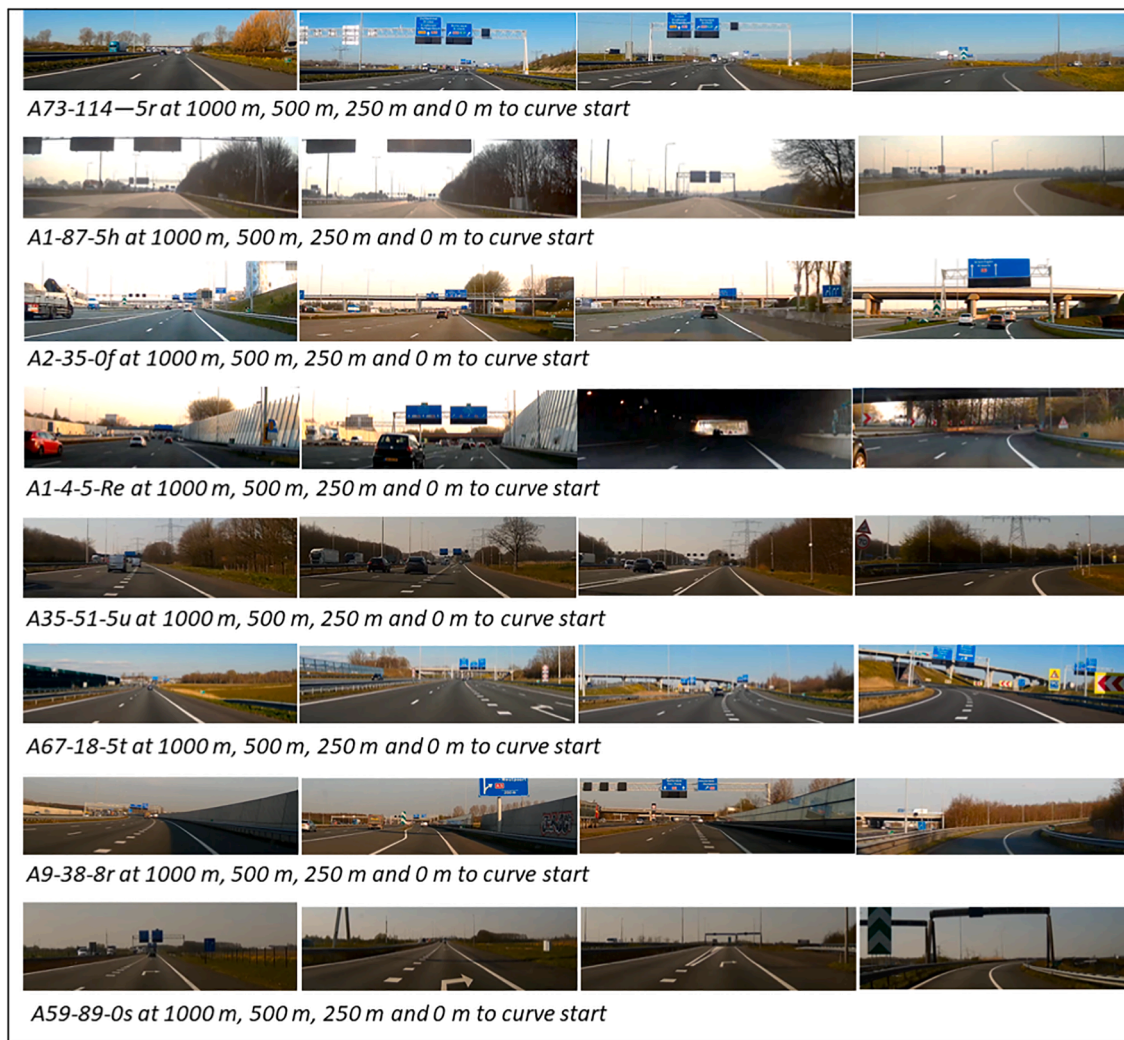


Fig. 6. Dashcam pictures of the actual carriageways taken at 1000 m (most left picture), 500 m, 250 m and 0 m (most right picture) to the curve start of each speed profile shown in Fig. 5.

were not found to correlate to the breakpoint variables.

3.3. Regression analysis

Regression analysis was used to explore the relationship between the positions and speeds of BP1 and BP2 and the explanatory variables. The horizontal radius of the curve is the defining variable of a curve. Fig. 8 clearly shows relations of the horizontal curve radius to the distance of BP1 and the speed at BP2. The position of BP2 is loosely correlated with the radius of the curve. The speed at BP1 is not correlated with the horizontal curve radius because it is assumed that drivers chose an optimal desired speed and are not being influenced by the horizontal radius, and indeed in Fig. 8C a very scattered plot is shown.

The formulas derived in Fig. 8 contribute to the prediction of the position and speed of BP1 and BP2 (respectively d_{BP1} and d_{BP2} in meters and v_{BP1} and v_{BP2} in km/h) for different horizontal curve radii (R_h) in meters. These formulas have been used to create mean speed profiles for an array of different horizontal radii as shown in Fig. 9. This shows the average speed behaviour in curve approach as a function of the horizontal radius of the curve, based on BP1 and BP2.

Each of the two breakpoints (BP1, BP2) shown as a mean in Fig. 9 has a variability in the relation to the horizontal radius as shown in Fig. 8. We have used linear regression analysis on all available variables, to investigate how much each variable explains the variability of BP1 and

BP2. We used the BIC value as an indicator for the fitness of the model. We started with a base model, showing the breakpoint as a function of the horizontal radius of the curve, as shown in Fig. 8. Next we created new models, in which we added one variable per model, to examine the contribution of this variable to explaining the variability. The added variables which lowered the BIC value of the base model by at least 0.05% showed that these variables could have a relevant contribution in explaining the variance of the breakpoints. Those variables were then checked for collinearity, before creating and testing multiple regression models. The outcome of these steps are presented in the next subsections.

3.3.1. Breakpoint 1 (BP1)

In Table 1 we show which variables contribute to predicting the distance of BP1 to curve start (d_{BP1}). Both the visible angle of the curve at BP1 (\angle_{BP1}) and the visible length of the curve at BP1 ($v_{LC_{BP1}}$) decrease the BIC value more than 2.9%, but are rather correlated, because the deflection angle is a derivative of curve radius and length. Because the closer a driver gets to a curve, the more length and deflection angle he can see, it is logical that the visible angle (\angle_{BP1}) is related to the position of BP1 (d_{BP1}). We chose to investigate the effect of the visible angle (\angle_{BP1}) further because it was found to decrease the BIC value more than the visible length of the curve, and is less obviously related to the distance of BP1 to the curve start. Next, the speed at BP1

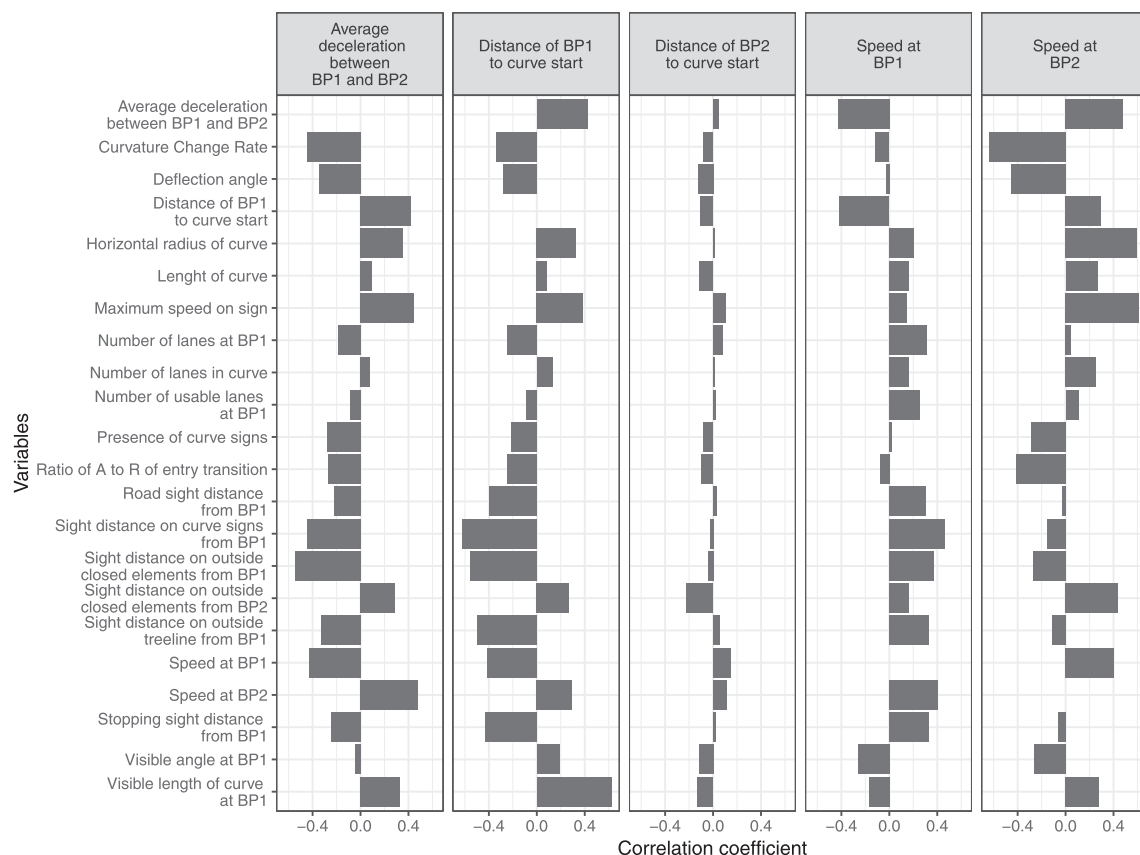


Fig. 7. Correlations between variables which determine speed profiles and variables which determine the curve.

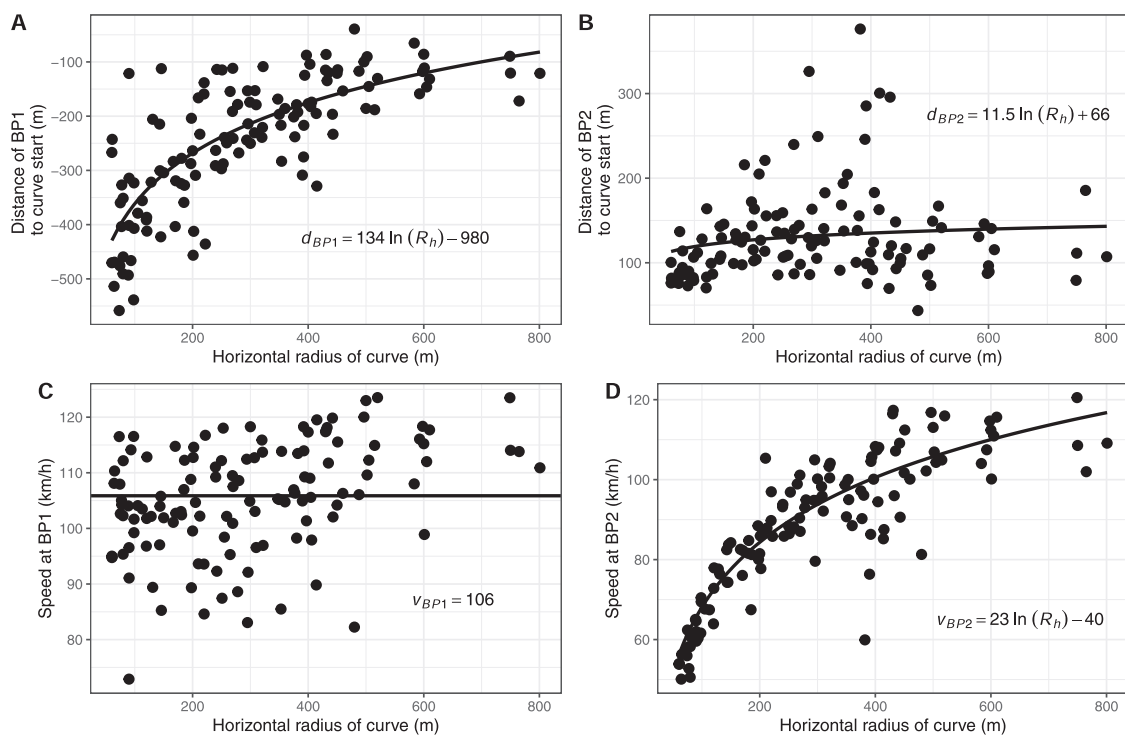


Fig. 8. Relations of the positions and speeds at BP1 and BP2 to the horizontal radius of the curve. Each point refers to the average value of a single curve for that variable.

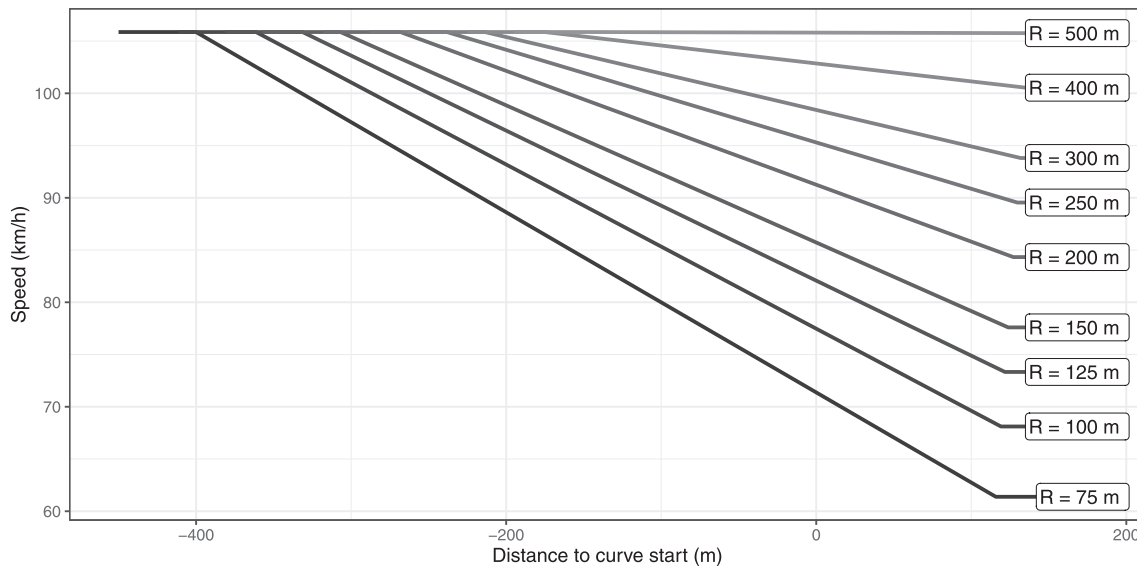


Fig. 9. Mean speed profiles for different horizontal radii, based on the mean positions and speeds at BP1 and BP2, derived from Fig. 8.

(v_{BP1}) was found to explain some of the variability in the distance of BP1 to curve start. This is because the faster a driver drives, the more length they need to decelerate. Both the road sight distance and stopping sight distance at BP1 (RSD_{BP1} and SSD_{BP1}) improve the explainability of the model, but since both sight distances are collinear, only one of the two variables will be considered. We explored the stopping sight distance (SSD_{BP1}) further because it decreased the BIC value most and is an internationally used measurement. The total number of lanes and the number of pre-sorting lanes to the curve, as well as the width of the carriageway at BP1 (nL_{BP1} , nuL_{BP1} , and W_{BP1}) are also correlated. We explored the total number of lanes (nL_{BP1}) further, because it reduced the BIC value most. The effect of not having all the lanes available because of pre-sorting at BP1, is covered in a variable checking the presence of a discontinuity. The presence of different types of discontinuities (weaving section, exit lane or a fork) at BP1 (W_{SBP1} , El_{BP1} and FO_{BP1} respectively) are correlated, so we chose to explore the variable of continuity at BP1 (C_{BP1}) further, because it lowers the BIC value most and covers the presence of discontinuity and the need for pre-sorting as well.

The selected variables in Table 1 were used to create multiple regression models for predicting the position of BP1. The results are shown in Table 2. This shows the added explainability of using sight and visibility in the model to predict the distance of BP1. Dropping the visible angle ($v\theta_{BP1}$) from the model, decreases the explainability drastically as seen in models 4 and 7 in Table 2. The models show that with more curve angle visible, the position of BP1 moves closer towards the curve start. But, with more sight distance (SSD_{BP1} and SD_{maxBP1}) available at BP1, this is located further away from the curve start. However, a sight on curve signs (CSS_{BP1}) decreases the distance of BP1 to the curve start. Fig. 10 shows how these sight distances interact with the position of BP1. Stopping Sight Distance from BP1 (SSD_{BP1}) is defined by how far ahead the driver is able to see a braking light. In most cases the SSD remains the roughly same if the position of BP1 changes. Whether or not a curve sign is visible from BP1 (CSS_{BP1}) is defined by whether or not BP1 is positioned beyond the point where the signs are visible the first time. If BP1 gets closer to the curve start from that point, the variable remains “yes”. The visible part of deflection angle seen from BP1 ($v\theta_{BP1}$) is very much related to the position of BP1 to the curve start. The closer BP1 is located to the curve start, the larger the visible deflection angle will be. Adding lanes (nL_{BP1}) to the cross section, increases the distance between BP1 and the curve start, and this is even more when a discontinuity (C_{BP1}) is added. Finally, during daytime (T) the position of BP1 is located closer to the curve start, than during night

time.

The speed at BP1 (v_{BP1}) is not correlated with the curve itself, but is used as a variable to define the position of BP1. So, no specific model has been created to define the speed at BP1. In case of consecutive curves, the speed at BP2 (v_{BP2}) for the first curve, can be used as the speed at BP1 (v_{BP1}) to predict the position of BP1 (d_{BP1}) for the second curve.

3.3.2. Breakpoint 2 (BP2)

As shown in Fig. 8B, the position of BP2 (d_{BP2}) is weakly correlated with the horizontal radius of the curve. The position is on average 135 m from the curve start, but varies between 50 and 350 m. Fig. 7 shows no variables correlate to the position of BP2. We found that different variables did not reduce the BIC by more than 0.15% compared to the base model. Curve length has no influence in this, since the curves in this study have an average length of 303 m ($sd = 46.5$ m). When investigating the curves which are causing the variability, we notice that the curves which have a position of BP2 beyond 160 m after curve start, all have follow-up curves which need further speed reduction. We can exclude these curves in our analysis on the position of BP2, since these positions are actually related to the consecutive curve. Hence we assume the position where drivers stop decelerating (d_{BP2}) is rather constant along different horizontal radii.

In Table 3 we show the variables added to the base model which contribute to the prediction of the speed at BP2. The speed at BP1 decreases the BIC of the base model most. Since the deflection angle of the curve and the entry transition curve (θ_c and θ_{etc} , respectively) as well as the Curvature Change Rate (CCR_{tot}) are collinear with the total deflection angle (θ_{tot}) we chose to explore this variable further. By doing so, we isolated the deflection angle, which is part of the calculation of the CCR. Also the total length of the curve (L_{tot}) and turning direction (Dir) are of influence. In the cross section, the presence of a discontinuity, number of lanes and the width of the emergency lane (C_{BP2} , nL and W_{el}) further lower the BIC. Finally, the presence of curve signs (pCS) also lowers the BIC of the base model.

The selected variables in Table 4 were used to create multiple regression models. The results are shown in Table 4. This shows that with a higher speed in front of the curve (v_{BP1}), a higher speed in the curve (v_{BP2}) is obtained. Furthermore, increasing length and angle of the curve (θ_{tot} and L_{tot}) seem to increase the speed in a curve. And, also, the wider the cross section gets, the higher the speed gets. However, adding the speed at BP1, deflection angle, length and direction of the curve (v_{BP1} , θ_{tot} , L_{tot} and Dir) to the model, nullifies this effect for the number of lanes in the curve (nL).

Table 1

Variables which increase the explainability of the position of BP1 (variables with an asterisk (*) are not explored further because of collinearity).

Added variable to $d_{BP1} = \ln(R_h) + \dots$	Variable Interpretation	model BIC	BIC decrease	Variable collinear with
vO_{BP1}	Visible angle of the curve at BP1 (grad) (see Vos et al. (2020))	19,339,426	2.97%	vLC_{BP1} (R (1481780) = 0.49, $p < .0001$)
vLC_{BP1}^*	Visible Length of the curve at BP1 (m)*	19,349,040*	2.92%*	VO_{BP1} (R (1481780) = 0.49, $p < .0001$)*
v_{BP1}	Speed at BP1 (km/h)	19,457,787	2.37%	
SSD_{BP1}	Stopping Sight Distance at BP1 (m)	19,605,067	1.64%	RSD_{BP1} (R (1481903) = -0.86, $p < .0001$)
RSD_{BP1}^*	Road Sight Distance at BP1 (m)*	19,632,363*	1.50%*	SSD_{BP1} (R (1481903) = -0.86, $p < .0001$)*
nL_{BP1}	Number of Lanes at BP1	19,798,294	0.67%	nUL_{BP1} (R (1481903) = -0.68, $p < .0001$), W_{BP1} (R (1481903) = -0.75, $p < .0001$)
W_{BP1}^*	Width of carriageway at BP1*	19,844,715*	0.43%*	nL_{BP1} (R (1481903) = -0.75, $p < .0001$), nUL_{BP1} (R (1481903) = -0.47, $p < .0001$)*
C_{BP1}	Continuity at BP1 (1 = continuous, 0 = discontinuous)	19,863,030	0.34%	FO_{BP1} (R (1481903) = -0.47, $p < .0001$), EL_{BP1} (R (1481903) = -0.41, $p < .0001$), WS_{BP1} (R (1481903) = -0.49, $p < .0001$)
CSS_{BP1}	Curve Sign in Sight at breakpoint 1 (1 = yes, 0 = no)	19,872,820	0.29%	
WS_{BP1}^*	Weaving section at breakpoint 1 (1 = weaving section, 0 = continuous or other discontinuity)*	19,888,209*	0.21%*	C_{BP1} (R (1481903) = -0.49, $p < .0001$)*
$SDmax_{BP1}$	Maximum Sight Distance at BP1 (m) (maximum of sight on road, stopping sight, guardrail, curve signs, treeline or closed elements)	19,895,226	0.18%	
nUL_{BP1}^*	Number of usable Lanes at breakpoint 1 based on pre-sorting; correct pre-sorting lanes leading up to the curve*	19,898,082*	0.17%*	nL_{BP1} (R (1481903) = -0.68, $p < .0001$), W_{BP1} (R (1481903) = -0.47, $p < .0001$)*
EL_{BP1}^*		19,898,961*	0.16%*	

Table 1 (continued)

Added variable to $d_{BP1} = \ln(R_h) + \dots$	Variable Interpretation	model BIC	BIC decrease	Variable collinear with
	Exit lane at breakpoint 1 (1 = exit lane, 0 = continuous or other discontinuity)*			C_{BP1} (R (1481903) = -0.41, $p < .0001$)*
FO_{BP1}^*	fork at breakpoint 1 ((1 = fork, 0 = continuous or other discontinuity)*	19,911,603*	0.10%*	C_{BP1} (R (1481903) = -0.47, $p < .0001$)*
T	Daytime (1 = sun up, 0 = sun down)	19,916,198	0.07%	

4. Discussion, limitations and future research directions

We have shown that the radius of a curve is of influence on the position where drivers start to decelerate in front of a curve, as well as the speed they select within a curve. We present a relation which shows when the horizontal radius decreases, drivers start decelerating further away from the curve. This deviates from the findings by Montella et al. (2015), who show drivers start decelerating closer to the curve, when the radius decreases. This difference might be explained by the use of a driving simulator in the study by Montella et al. (2015) and the distortion of a curve from a driver's standpoint (Brummelaar, 1975) in such an experiment. This strengthens the hypothesis that drivers on freeways use other cues besides the horizontal radius alone to select their speed.

This research focusses on the positions where 0 m/s² was reached in speed profiles. These positions however do not match up with the perceptual tasks, since the breakpoints are preceded by the cognitive and psychomotor tasks (Campbell et al., 2012; Shinar, 2017). The cues drivers actually react to, could be present up to a couple of seconds before the position where 0 m/s² is reached.

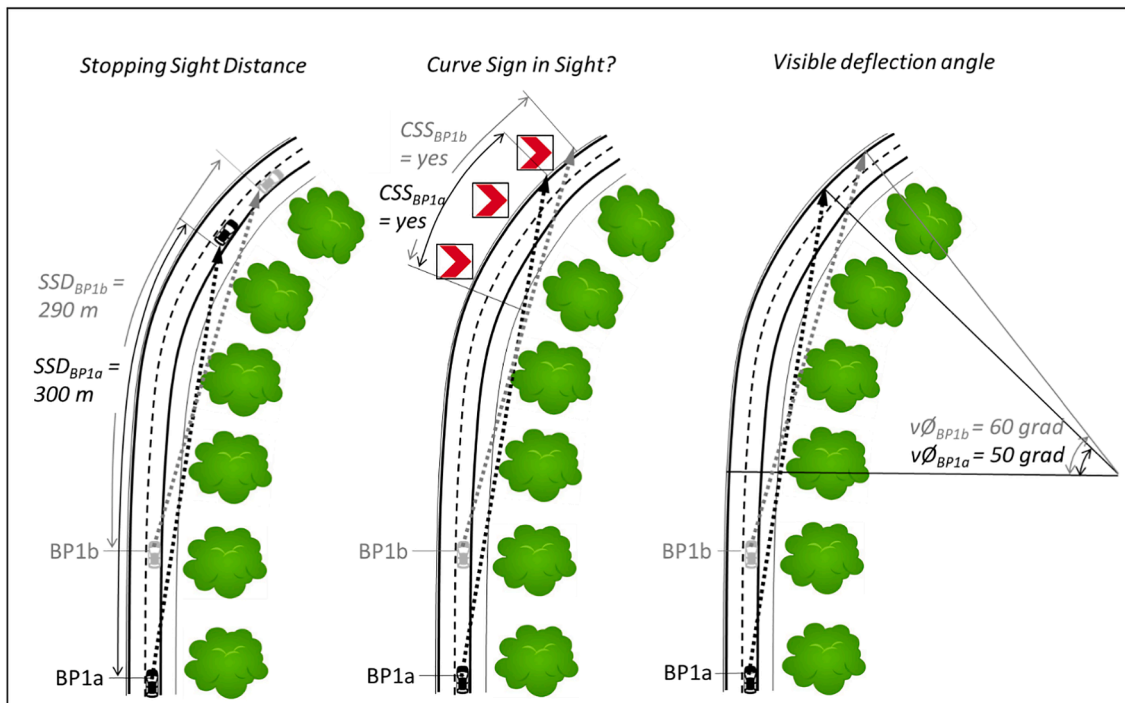
The amount of visibility of the curve at BP1 is correlated with the position of BP1. It remains unclear however whether this is a cause or an effect, because the closer BP1 is positioned to the curve start, the more of that curve the driver would be able to see. So, visibility-variables which take the position of the curve start into account (e.g. visible angle or curve sign in sight) should not be taken into account in explaining the position of BP1. This means that the need to recognise 100 m of the curve (Campbell et al., 2012; ROA, 2019) cannot be underpinned by this study. The focus should be on the sight distances though, which show that if a driver has increased sight distances available, deceleration occurs earlier. Effects of individual guiding elements were not found, although adding guiding elements to the sight distance ($SDmax_{BP1}$) increases this effect. The finding that stopping sight distance (SSD_{BP1}) added more explainability to the regression analysis of the position of BP1 (d_{BP1}) than the road sight distance (RSD_{BP1}) could be explained because SSD analysis in 'Zicht' created a smoother line than RSD analysis because it is less prone to sight obstructions. This adds to the thought that drivers need continuous information (Coutton-Jean et al., 2009; Singh and Fulvio, 2007). The presence of curve signs only correlates to the position of BP1, when these are tested on correlation in Fig. 7. But when added in a regression model together with horizontal radius it shows no extra explainability, other than the speed at BP2 (v_{BP2}).

The cross section is of influence both on the position where deceleration starts (BP1), as well as the speed in a curve. Increasing the width of a cross section, increases the distance of BP1 from the curve start. This could be explained by the speed at BP1, however this was not collinear. One explanation could be the extra perceived risk with multiple lanes in a cross section (Vos et al., 2020), which could lead the driver to decelerate more cautiously. But, because we tested only speed profiles in free flow situations, this explanation is unlikely, since not much other vehicles should be around during the measurement. The addition of pre-

Table 2

Regression analysis results for the position of BP1.

	Model 1 (base)	Model 2	Model 3	Model 4	Model 5	Model 6	Model 7
Constant	−980.286*** (1.629) *	−1104.617*** (1.166)	−1115.862*** (1.235)	−934.521*** (1.586)	−965.670*** (1.299)	−947.848*** (1.263)	−495.498*** (1.481)
$\ln(R_h)$	134.395*** (0.289)	180.308*** (0.194)	182.810*** (0.202)	138.395*** (0.278)	192.028*** (0.197)	191.076*** (0.196)	155.613*** (0.236)
$v\phi_{BP1}$		2.852*** (0.002)	2.829*** (0.003)		2.448*** (0.003)	2.449*** (0.003)	
v_{BP1}					−2.269*** (0.006)	−2.308*** (0.006)	−4.166*** (0.008)
SSD_{BP1}		−0.826*** (0.001)	−0.792*** (0.001)		−0.650*** (0.001)	−0.650*** (0.001)	−0.457*** (0.001)
$SD_{max_{BP1}}$			−0.043*** (0.000)		−0.038*** (0.000)	−0.038*** (0.000)	−0.027*** (0.000)
CSS_{BP1}			19.756*** (0.276)		21.669*** (0.264)	21.010*** (0.264)	
nL_{BP1}				−42.137*** (0.147)	−3.798*** (0.101)	−4.366*** (0.100)	−14.986*** (0.128)
C_{BP1}				48.093*** (0.386)	14.982*** (0.253)	13.978*** (0.253)	43.465*** (0.322)
T					12.004*** (0.209)	11.344*** (0.268)	
Num.Obs.	1,481,905	1,481,905	1,481,905	1,481,905	1,481,905	1,481,905	1,481,905
R2	0.127	0.629	0.635	0.210	0.669	0.668	0.457
R2 Adj.	0.127	0.629	0.635	0.210	0.669	0.668	0.457
AIC	19931003.8	18664030.3	18640587.0	19782830.0	18493508.1	18496798.2	19227773.9
BIC	19931040.4	18664091.3	18640672.5	19782891.1	18493642.4	18496920.3	19227883.8
Log.Lik.	−9965498.884	−9332010.129	−9320286.511	−9891410.008	−9246743.040	−9248389.087	−9613877.949
F	215655.159	836516.766	514640.655	131390.746	332926.431	373300.302	178081.226

* $p < 0.1$, ** $p < 0.05$, *** $p < 0.01$.**Fig. 10.** Sightlines from BP1 are shown in two different positions of BP1 (a and b) as a dotted arrow to show the effect on different sight distance measurements.

sorting tasks effects increase this effect. Having a discontinuity at breakpoint 1, increases the distance to the curve start even more. The speed in a curve decreases with the addition of extra lanes, but only if the length and angle of the curve are taken into account. When analysing the number of lanes in a curve without any other variables, the increasing number of lanes increases speed in a curve, just as Calvi et al. (2018) also showed. Our study shows the impact of other variables of the curve on this effect. One of these effects is the direction of the curve. We

show that in right turning curves the speed is higher than in left turning curves, which is not in line with the findings of Farah et al. (2019) but is in line with findings of Misaghi and Hassan (2005). Since more visual attention is towards the right in right turning curves compared to the left in left turning curves (Lappi and Lehtonen, 2013; Shinar et al., 1977), but no sight distances added explainability to the speed at breakpoint 2, it remains unclear as to why drivers drive faster in right turning curves. However, since all the afore mentioned studies

Table 3

Variables which increase the explainability of the position of BP1 (variables with an asterisk (*)) are not explored further because of collinearity).

Added variable to $v_{BP2} = \ln(R_h) + \dots$	Variable Interpretation	model BIC	BIC decrease	Variable collinear with
v_{BP1}	Speed at BP1 (km/h)	12,049,030	1.96%	
θ_c^*	Deflection angle of the horizontal curve (rad)*	12,269,707*	0.17%*	θ_{tot} (R (1481903) = 0.98, $p < .0001$) CCR_c (R (1481903) = 0.63, $p < .0001$)*
θ_{tot}	Total deflection angle of the horizontal curve, including transition curves (rad)	12,269,917	0.16%	θ_{etc} (R (1481903) = 0.83, $p < .0001$) θ_c (R (1481903) = 0.98, $p < .0001$) CCR_{tot} (R (1481903) = 0.80, $p < .0001$)
L_{tot}	Total Length of the horizontal curve, including transition curves (m)	12,272,569	0.14%	L_c (R (1481903) = 0.94, $p < .0001$)
C_{BP2}	Continuity at BP2 (1 = continuous, 0 = discontinuous)	12,274,609	0.13%	
nL	number of Lanes in curve	12,274,036	0.13%	W (R (1481903) = 0.74, $p < .0001$) CCR_c (R (1481903) = 0.98, $p < .0001$) θ_{tot} (R (1481903) = 0.80, $p < .0001$)*
CCR_{tot}^*	Total Curvature Change Rate of horizontal curve, including transition curves*	12,276,095*	0.11%*	i (R (1481903) = 0.78, $p < .0001$) CCR_{tot} (R (1481903) = 0.98, $p < .0001$) θ_c (R (1481903) = 0.63, $p < .0001$)*
Dir	Direction of curve (1 = right turning, -1 = left turning)	12,276,473	0.11%	θ_{etc} (R (1481903) = 0.83, $p < .0001$)*
CCR_c^*	Curvature Change Rate of horizontal curve*	12,277,515*	0.10%*	nL (R (1481903) = 0.74, $p < .0001$)*
θ_{etc}^*	Deflection angle of entry transition curve (rad)*	12,278,122*	0.10%*	L_{tot} (R (1481903) = 0.94, $p < .0001$)
W^*	Width of carriageway in curve (m)*	12,277,702*	0.10%*	A_{etc} R (1481903) = 0.77, $p < .0001$)*
L_c	Length of horizontal curve (m)	12,279,619	0.09%	Dir (R (1481903) =
L_{etc}^*	Length of entry transition curve (m)*	12,279,271*	0.09%*	
i^*	Superelevation in curve (%)*	12,281,303*	0.07%*	

Table 3 (continued)

Added variable to $v_{BP2} = \ln(R_h) + \dots$	Variable Interpretation	model BIC	BIC decrease	Variable collinear with
W_{el}	Width of emergency lane (m)	12,283,065	0.06%	0.78, $p < .0001$)*
A_{etc}^*	A-value of entry transition curve (clothoid parameter)*	12,283,939*	0.05%*	L_{etc} R (1481903) = 0.77, $p < .0001$)*
pCS	Presence of curve signs in curve (1 = yes, 0 = no)	12,283,822	0.05%	

were undertaken in right driving countries, it could have to do with the added visibility of the curve trajectory, because it is less obscured by the bodywork of the car.

The relation between the radius and start of deceleration shows an increase in variability of the position of BP1 when the radius decreases. This heteroscedasticity is explained mostly by the speed at BP1, the larger the radius of a curve, the less speed adjustment is needed. The relation of radius and the speed in a curve shows a decrease in variability of the speed at BP2 if the radius decreases. This shows that the smaller a radius gets, the less speed in a curve is influenced by other variables than the horizontal radius.

By using all individual speed profiles in the statistical analysis, we were able to gain insight in individual speed choices. This showed a positive correlation between the speed before a curve, and inside a curve, suggesting that fast drivers on tangents, also drive fast through curves. This could relate to individual driving style or familiarity. Since speed before a curve is important to the speed in a curve, speed prediction models should pay more attention to elements which influence speed before a curve, such as discontinuities. [Hassan et al. \(2011a\)](#) already noted that both upstream and downstream elements influence measurements at a certain location.

No correlation to the vertical alignment was found in this study. This could be related to the relatively large sag curves in the data-set, so critical combinations are almost not present in the data. This could also be due to the relative flatness of most road sections in the Netherlands, which could also explain why the grade of the road did not correlate with any breakpoint as well.

The amount of precipitation has no substantial influence on the position of BP1, or the speed at BP2, and therefore not on deceleration. Wet surfaces offer less friction ([Donnell et al., 2016](#); [Li and He, 2016](#)) and therefore lead to increased crash risks. This increased risk seems not to influence speed behaviour. A small correlation to daylight and breakpoint 1 is seen. Drivers tend start decelerating later in daylight, suggesting a more cautious curve approach in lessened visibility, the effect is however less than half a second.

The sample of drivers used in this research appear to be faster drivers than the average driver in the Netherlands. This might also indicate a higher level of experience and familiarity, and could also be an explanation for not finding relations to precipitation. This should be kept in mind when translating these insights into design-policy or safety assessments. The use of this set of faster drivers represents a subset which is willing to take a higher risk of skidding than the average driver.

The use of High Frequency Floating Car data is promising, but this data is not readily available because regular Floating Car Data recording methods need to be altered into a higher data gathering frequency within the used apps. This includes careful consideration of research purposes and selecting useful road sections in future research using this type of data. Because the data has high frequency time series, using complex functional data analysis could give more multi-dimensional insights ([Ramsay et al., 2009](#)).

Table 4

Regression analysis results for the speed at BP2.

	Model 1 (base)	Model 2	Model 3	Model 4	Model 5	Model 6	Model 7
<i>Constant</i>	−39.609*** (0.124)	−54.003*** (0.130)	−48.737*** (0.135)	−60.448*** (0.124)	−37.843*** (0.140)	−43.345*** (0.147)	−45.276*** (0.160)
$\ln(R_h)$	23.391*** (0.022)	19.770*** (0.022)	18.124*** (0.025)	21.041*** (0.021)	22.386*** (0.023)	17.458*** (0.025)	17.804*** (0.028)
v_{BP1}		0.331*** (0.001)	0.337*** (0.001)	0.318*** (0.001)		0.353*** (0.001)	0.351*** (0.001)
θ_{tot}		0.020*** (0.000)	0.040*** (0.000)			0.038*** (0.000)	0.039*** (0.000)
L_{tot}			0.006*** (0.000)	0.002*** (0.000)		0.008*** (0.000)	0.008*** (0.000)
<i>Dir</i>			3.385*** (0.026)	−1.214*** (0.014)		3.222*** (0.026)	3.333*** (0.026)
nL					1.869*** (0.018)	−0.234*** (0.017)	−0.307*** (0.017)
C_{BP2}					−4.531*** (0.044)	−9.227*** (0.041)	−9.229*** (0.041)
W_{el}					1.429*** (0.017)	1.236*** (0.016)	1.240*** (0.016)
pCS							0.913*** (0.030)
Num.Obs.	1,481,905	1,481,905	1,481,905	1,481,905	1,481,905	1,481,905	1,481,905
R2	0.433	0.531	0.536	0.523	0.446	0.554	0.554
R2 Adj.	0.433	0.531	0.536	0.523	0.446	0.554	0.554
AIC	12290097.4	12010287.7	11992963.6	12034897.2	12256647.7	11935478.1	11934563.4
BIC	12290134.1	12010348.7	11993049.1	12034970.5	12256720.9	11935600.2	11934697.7
Log.Lik.	−6145045.720	−6005138.838	−5996474.811	−6017442.606	−6128317.830	−5967729.064	−5967270.703
F	1133386.776	558968.079	342810.984	406220.801	298274.797	230059.611	204725.726

* $p < 0.1$, ** $p < 0.05$, *** $p < 0.01$.

The discussion showed uncertainty in causality for the relation between visibility and the position where drivers start decelerating. Further research on where the visual focus of drivers lies just before deceleration, could give better insights into the cues which drivers use to start decelerating. Using two time dependent variables – visual focus and start of deceleration – could infer a causal relation between the guiding element which was focussed on by the driver and the deceleration which occurred, using knowledge about the drivers information processing (Shinar, 2017).

5. Conclusions

We were able to show that the distance to a curve start where drivers start to decelerate is related to the horizontal radius of that curve, and this result confirms earlier findings that speed in the curve is also related to the horizontal radius. We found relations of the driven speed in front of the curve to the speed behaviour in curve approach and concluded that drivers stop decelerating at around 135 m into the curve independent from the horizontal radius and speed.

So, horizontal radius is a key characteristic for a curve and the speed behaviour upon curve entry. Variability in positions where drivers start to decelerate are explained further by stopping sight distances, number of lanes, the presence of a discontinuity for pre-sorting and daylight. We were unable to find relations towards specific guiding elements in a curve which determine speed behaviour in front of a curve, other than the presence of curve signs.

The speed in a curve is further explained by the deflection angle and length of a curve, as well as the direction of the curve. Also the cross section is of influence, but we were unable to provide good explanation to the relation of the number of lanes, width of the emergency lane and discontinuities with the speed inside the curve. Of further interest is that sight distances do not seem to influence speed within a curve.

Given the insights gained in this research, freeway curve design should not be solely based on side friction, but should take actual speed behaviour into account as well. This means considering the existence of deceleration in a constant circular curve, and acknowledging the influence of upstream road characteristics and other curve characteristics on

speed behaviour upon a curve. This could reveal differences in friction demand based on actual speed behaviour. Furthermore, problems regarding to speeding and traffic safety in curves, can be analysed using the variables in this research.

Funding

The acquisition of the reverse engineered road sections and the High Frequency Floating Car Data was funded by Rijkswaterstaat (Dutch Directorate-General for Public Works and Water Management).

CRedit authorship contribution statement

Johan Vos: Conceptualization, Methodology, Software, Validation, Formal analysis, Investigation, Data curation, Writing - original draft, Visualization, Project administration, Funding acquisition. **Haneen Farah:** Conceptualization, Methodology, Writing - review & editing, Supervision. **Marjan Hagenzieker:** Writing - review & editing, Supervision.

Declaration of Competing Interest

The authors declare that they have no known competing financial interests or personal relationships that could have appeared to influence the work reported in this paper.

References

- Bella, F., 2009. Can driving simulators contribute to solving critical issues in geometric design? Transp. Res. Rec. 2138, 120–126. <https://doi.org/10.3141/2138-16>.
- Bella, F., 2014. Driver performance approaching and departing curves: driving simulator study. Traffic Inj. Prev. 15 (3), 310–318. <https://doi.org/10.1080/15389588.2013.813022>.
- Bella, F., 2015. Coordination of horizontal and sag vertical curves on two-lane rural roads: driving simulator study. IATSS Res. 39 (1), 51–57. <https://doi.org/10.1016/j.iatssr.2015.02.002>.
- Blumentrath, C., Tveit, M.S., 2014. Visual characteristics of roads: a literature review of people's perception and Norwegian design practice. Transportation Res. Part A: Policy Pract. 59, 58–71. <https://doi.org/10.1016/j.tra.2013.10.024>.

- Broeren, P., 2002. Evaluating sight distances in highway design, a practical tool. Paper presented at the TRB Symposium on Visualization in Transportation, Salt Lake City.
- Brummelaar, T.T., 1975. Where are the kinks in the alignment? *Transp. Res. Rec.* 556, 35–50.
- Calvi, A., Bella, F., D'Amico, F., 2018. Evaluating the effects of the number of exit lanes on the diverging driver performance. *J. Transp. Saf. Secur.* 10 (1–2), 105–123. <https://doi.org/10.1080/19439962.2016.1208313>.
- Campbell, J.L., Lichty, M.G., Brown, J.L., Richard, C.M., Graving, J.S., et al., 2012. Human factors guidelines for road systems, second ed. Transportation Research Board, Washington, D.C.
- Charlton, S.G., 2004. Perceptual and attentional effects on drivers' speed selection at curves. *Accid. Anal. Prev.* 36 (5), 877–884. <https://doi.org/10.1016/j.aap.2003.09.003>.
- Charlton, S.G., Starkey, N.J., 2013. Driving on familiar roads: automaticity and inattention blindness. *Transp. Res. Part F: Traffic Psychol. Behav.* 19, 121–133. <https://doi.org/10.1016/j.trf.2013.03.008>.
- Charlton, S.G., Starkey, N.J., 2017a. Drivers' mental representations of familiar rural roads. *J. Environ. Psychol.* 50, 1–8. <https://doi.org/10.1016/j.jenvp.2017.01.003>.
- Charlton, S.G., Starkey, N.J., 2017b. Driving on urban roads: how we come to expect the 'correct' speed. *Accid. Anal. Prev.* 108, 251–260. <https://doi.org/10.1016/j.aap.2017.09.010>.
- Cleveland, W.S., Grosse, E., Shyu, W.M., 1992. Local regression models. *Statistical Models in S*: Routledge.
- Cohen, J., 1988. Statistical power analysis for the behavioral sciences, second ed. Routledge, New York.
- Colombaroni, C., Fusco, G., Isaenko, N., 2020. Analysis of road safety speed from floating car data. Paper presented at the Transportation Research Procedia.
- Coutton-Jean, C., Mestre, D.R., Goulon, C., Bootsma, R.J., 2009. The role of edge lines in curve driving. *Transp. Res. Part F: Traffic Psychol. Behav.* 12 (6), 483–493. <https://doi.org/10.1016/j.trf.2009.04.006>.
- de Waard, D., Steyvers, F.J.J.M., Brookhuis, K.A., 2004. How much visual road information is needed to drive safely and comfortably? *Saf. Sci.* 42 (7), 639–655. <https://doi.org/10.1016/j.ssci.2003.09.002>.
- Dias, C., Oguchi, T., Wimalasena, K., 2018. Drivers' speeding behavior on expressway curves: exploring the effect of curve radius and desired speed. *Transp. Res. Rec.* 2672, 48–60. <https://doi.org/10.1177/0361198118778931>.
- Donnell, E., Wood, J., Himes, S., Torbic, D., 2016. Use of side friction in horizontal curve design: a margin of safety assessment. *Transp. Res. Rec.* 2588, 172–180. <https://doi.org/10.3141/2588-07>.
- Farah, H., Daamen, W., Hoogendoorn, S., 2019. How do drivers negotiate horizontal ramp curves in system interchanges in the Netherlands? *Saf. Sci.* 119, 58–69. <https://doi.org/10.1016/j.ssci.2018.09.016>.
- Fildes, B.N., Triggs, T.J., 1985. The on effect of changes in curve geometry magnitude estimates of road-like perspective curvature. *Perception Psychophys.* 37 (3), 218–224.
- Fitzpatrick, K., Kahl, K., 1992. A Historical and Literature Review of Horizontal Curve Design. Texas Transportation Institute, Austin, Texas.
- Gibson, J.J., Crooks, L.E., 1938. A theoretical field-analysis of automobile-driving. *Am. J. Psychol.* 51 (3), 453. <https://doi.org/10.2307/1416145>.
- Gruppelaar, V., Paassen, R.V., Mulder, M., Abbink, D., 2018. A perceptually inspired driver model for speed control in curves. Paper presented at the 2018 IEEE International Conference on Systems, Man, and Cybernetics (SMC).
- Hallmark, S., Oneyear, N., Wang, B., Tyner, S., Carney, C., McGehee, D., 2015. Identifying curve reaction point using NDS data. Paper presented at the IEEE Conference on Intelligent Transportation Systems.
- Hashim, I.H., 2011. Analysis of speed characteristics for rural two-lane roads: A field study from Minoufiya Governorate, Egypt. *Ain Shams Eng. J.* 2 (1), 43–52. <https://doi.org/10.1016/j.asej.2011.05.005>.
- Hassan, Y., Sarhan, M., Dimaiuta, M., 2011a. Deficiencies in existing speed models. Modeling Operating Speed: Synthesis Report. Transportation Research Board, Washington, D.C.
- Hassan, Y., Sarhan, M., Porter, R., Dimaiuta, M., Donnell, E., Garcia, A., et al., 2011b. Modeling Operating Speed: Synthesis Report. Transportation Research Board, Washington, D.C.
- Hazenbergh, S.J., van Lier, R., 2016. Disentangling effects of structure and knowledge in perceiving partly occluded shapes: an ERP study. *Vision Res.* 126, 109–119. <https://doi.org/10.1016/j.visres.2015.10.004>.
- Hills, B.L., 1980. Vision, visibility, and perception in driving. *Perception* 9 (2), 183–216. <https://doi.org/10.1068/p090183>.
- Himes, S., Porter, R.J., Hamilton, I., Donnell, E., 2019. Safety evaluation of geometric design criteria: horizontal curve radius and side friction demand on rural, two-lane highways. *Transp. Res. Rec.* 2673, 516–525. <https://doi.org/10.1177/0361198119835514>.
- Jamson, S., Benetou, D., Tate, F., 2015. The impact of arc visibility on curve negotiation. *Adv. Transp. Stud.* 2015 (37), 79–92.
- Land, M.F., Lee, D.N., 1994. Where we look when we steer. *Nature* 369 (6483), 742–744. <https://doi.org/10.1038/369742a0>.
- Lappi, O., Lehtonen, E., 2013. Eye-movements in real curve driving: pursuit-like optokinetic in vehicle frame of reference, stability in an allocentric reference coordinate system. *J. Eye Movement Res.* 6 (1), 1–13.
- Lehtonen, E., Lappi, O., Koirikivi, I., Summala, H., 2014. Effect of driving experience on anticipatory look-ahead fixations in real curve driving. *Accid. Anal. Prev.* 70, 195–208. <https://doi.org/10.1016/j.aap.2014.04.002>.
- Lehtonen, E., Lappi, O., Summala, H., 2012. Anticipatory eye movements when approaching a curve on a rural road depend on working memory load. *Transp. Res. Part F: Traffic Psychol. Behav.* 15 (3), 369–377. <https://doi.org/10.1016/j.trf.2011.08.007>.
- Li, P., He, J., 2016. Geometric design safety estimation based on tire-road side friction. *Transp. Res. Part C: Emerg. Technol.* 63, 114–125. <https://doi.org/10.1016/j.trc.2015.12.009>.
- Llopis-Castelló, D., González-Hernández, B., Pérez-Zuriaga, A.M., García, A., 2018. Speed prediction models for trucks on horizontal curves of two-lane rural roads. In: *Transportation Research Record*, pp. 72–82.
- Luque, R., Castro, M., 2016. Highway geometric design consistency: speed models and local or global assessment. *Int. J. Civ. Eng.* 14 (6), 347–355. <https://doi.org/10.1007/s40999-016-0025-2>.
- McKnight, A.J., Adams, B.B., 1970. Driver education task analysis. Volume I: task descriptions. Final report.
- Misaghi, P., Hassan, Y., 2005. Modeling operating speed and speed differential on two-lane rural roads. *J. Transp. Eng.* 131 (6), 408–418. [https://doi.org/10.1061/\(ASCE\)0733-947X\(2005\)131:6\(408\)](https://doi.org/10.1061/(ASCE)0733-947X(2005)131:6(408)).
- Molino, J.A., Opiela, K.S., Katz, B.J., Moyer, M.J., 2005. Validate First; Simulate Later: A New Approach Used at the FHWA Highway Driving Simulator. North America, 10.
- Montella, A., Galante, F., Mauriello, F., Aria, M., 2015. Continuous speed profiles to investigate drivers' behavior on two-lane rural highways. *Transp. Res. Rec.* 2521 (1), 3–11.
- Odams, A.M., Cole, D.J., 2004. Models of driver speed choice in curves. Paper presented at the AVEC '04.
- Perco, P., 2006. Desirable length of spiral curves for two-lane rural roads. *Transp. Res. Rec.* 19. *J. Transp. Res. Board* 1961, 1–8. <https://doi.org/10.3141/1961-01>.
- Ramsay, J.O., Hooker, G., Graves, S., 2009. Functional Data Analysis with R and MATLAB. Springer-Verlag, New York.
- Riemersma, J.B.J., 1988. The Perception of Curve Characteristics. Instituut voor Zintuigfysiologie, Soesterberg.
- Riemersma, J.B.J., 1989. The effects of transition curves and superelevation on the perception of road-curve characteristics. Soesterberg, Institute for Perception.
- ROA - Rijkswaterstaat Ontwerp Autosnelwegen 2019. (Rijkswaterstaat Ed.). Utrecht: Rijkswaterstaat - Grote Projecten en Onderhoud.
- Saltikoff, E., Friedrich, K., Soderholm, J., Lengfeld, K., Nelson, B., Becker, A., et al., 2019. An overview of using weather radar for climatological studies: successes, challenges, and potential. *Bull. Am. Meteorol. Soc.* 100 (9), 1739–1752. <https://doi.org/10.1175/bams-d-18-0166.1>.
- Salvucci, D.D., Gray, R., 2004. A two-point visual control model of steering. *Perception* 33 (10), 1233–1248. <https://doi.org/10.1068/p5343>.
- Shinar, D., 2017. 5. Driver information processing: attention, perception, reaction time, and comprehension. *Traffic Safety and Human Behavior*, second ed. Emerald, Inc.
- Shinar, D., McDowell, E.D., Rockwell, T.H., 1977. Eye movements in curve negotiation. *Hum. Factors* 19 (1), 63–71.
- Singh, M., Fulvio, J.M., 2007. Bayesian contour extrapolation: geometric determinants of good continuation. *Vision Res.* 47 (6), 783–798. <https://doi.org/10.1016/j.visres.2006.11.022>.
- Sivak, M., 1996. The information that drivers use: is it indeed 90% visual? *Perception* 25 (9), 1081–1089. <https://doi.org/10.1068/p251081>.
- Van Winsum, W., Godthelp, H., 1996. Speed choice and steering behavior in curve driving. *Hum. Factors* 38 (3), 434–441. <https://doi.org/10.1518/001872096778701926>.
- Vos, J., Farah, H., Hagenzieker, M., 2020. How do dutch drivers perceive horizontal curves on freeway interchanges and which cues influence their speed choice? *IATSS Res.* <https://doi.org/10.1016/j.iatssr.2020.11.004>.
- Wang, F., Easa, S.M., 2009. Validation of perspective-view concept for estimating road horizontal curvature. *J. Transp. Eng.* 135 (2), 74–80.
- Wang, X., Guo, Q., Tarko, A.P., 2020. Modeling speed profiles on mountainous freeways using high resolution data. *Transp. Res. Part C: Emerg. Technol.* 117 <https://doi.org/10.1016/j.trc.2020.102679>.
- Wu, J., Xu, H., 2018. The influence of road familiarity on distracted driving activities and driving operation using naturalistic driving study data. *Transp. Res. Part F: Traffic Psychol. Behav.* 52, 75–85. <https://doi.org/10.1016/j.trf.2017.11.018>.